Protocol assessment for flow and shear stress applications in 3D microfluidic hydrogel-based 'vessel-on-a-chip' systems

Bachelor Assignment

Author: **R. Timmerije**

Assignment Committee:
Daily supervisor: **L.E. de Heus MSc**
Committee chair: **dr. A.D. van der Meer**
External committee member: **dr.ir. J. Rouwkema**

UNIVERSITY OF TWENTE. | TECHMED CENTRE

AST APPLIED STEM CELL TECHNOLOGIES

.

Protocol assessment for flow and shear stress applications in 3D microfluidic hydrogel-based 'vessel-on-a-chip' systems

Rick Timmerije

Enschede, June 30, 2021

Bachelor Assignment at the research group Applied Stem Cell Technologies

Part of Technical Medical Centre, University of Twente

Abstract

English

Three dimensional(3D) microfluidic hydrogel-based vessel-on-a-chip systems are increasingly used in research regarding cardiovascular physiology, pathophysiology and therapeutic drugs. Fluid flow and wall shear stress are important factors in regulation of the physiology of the vessel and disease progression. Currently, no protocol is present at the AST research group to test these factors inside the 3D hydrogel-based vessel-on-chip systems. The goal was to produce a workable and suitable protocol to apply flow inside the vessel-on-a-chip system. The developed protocol was validated by assessing the flow profile and finally applied in a vessel-on-a-chip seeded with endothelial cells. The obtained flow profile has a parabolic shape as expected. However, the flow rate deviated from the set flow rate, making exact shear stress calculations unpredictable. Next, flow was applied to endothelial cells to generate a physiologically relevant arterial shear stress for 6 hours. The protocol used in the assessment of the flow was limited to 200μL volume, which was not enough to apply a physiological shear stress for the set amount of time. A flow rate of 1.8mL/min was administered to generate 4.1 and 6.0 Pa of shear stress on the endothelial cells. To accommodate for this volume a protocol was proposed using a 50mL tube as reservoir. However, this protocol was very laborious in reusing the fluid. After applying the shear stress, the endothelial cells showed a orientation bias in the direction of the flow. The assessed protocol shows a characteristic flow profile and is capable of applying physiologically relevant arterial shear stresses, which induced a cellular response in endothelial cells.

Nederlands

Driedimensionale(3D) microfluïdische hydrogel-gebaseerde bloedvat-op-een-chip systemen worden steeds vaker gebruikt in onderzoek met betrekking tot cardiovasculaire fysiologie, pathofysiologie en therapeutische geneesmiddelen. Vloeistofstroom en afschuifspanning zijn belangrijke factoren bij de regulering van de fysiologie van het vat en de progressie van ziekten. Momenteel is er geen protocol beschikbaar bij de AST-onderzoeksgroep om deze factoren te testen in 3D hydrogel-gebaseerde bloedvat-op-chip systemen. Het doel was om een protocol te produceren dat geschikt en makkelijk in gebruik is om zo stroming toe te passen. Het ontwikkelde protocol werd gevalideerd door het stromingsprofiel te beoordelen en daarna toe te passen in een bloedvat-op-een-chip gezaaid met endotheelcellen. Het verkregen stromingsprofiel had een parabolische vorm, zoals verwacht. Het debiet wijkt echter af van het ingestelde debiet, waardoor exacte berekeningen van de afschuifspanning onvoorspelbaar zijn. Vervolgens werd flow toegepast om gedurende 6 uur een fysiologisch relevante arteriële afschuifspanning te genereren op endotheelcellen. Het protocol dat werd gebruikt bij de beoordeling van de stroming is gelimiteerd tot een volume van 200μL. Dit was niet genoeg was om een fysiologische afschuifspanning toe te passen gedurende de ingestelde tijd. Een stroomsnelheid van 1,8 mL/min werd toegediend om 4,1 en 6,0 Pa afschuifspanning op de endotheelcellen te genereren. Om rekening the houden met het benodigde volume werd een protocol voorgesteld met een 50mL buis als reservoir. Dit protocol was echter zeer arbeidsintensief en omslachtig bij het hergebruik van de vloeistof. Nadat de endotheelcell blootgesteld waren aan de afschuifspanning toonden ze een oriëntatie verandering in de richting van de stroming. Het voorgestelde protocol vertoont een karakteristiek stromingsprofiel en is in staat fysiologisch relevante arteriële afschuifspanningen toe te passen, die een cellulaire respons in endotheelcellen induceerde.

Contents

1 Introduction **4**

2 Theory **5**
2.1 Blood Vessels *in vivo* . . . 5
2.2 3D vessel-on-a-chip . . . 5
2.3 Pressure-driven Flow . . . 6
2.3.1 Laminar and turbulent flow . . . 6
2.3.2 Flow profile . . . 6
2.3.3 Active Pumping . . . 6
2.3.4 Fluid Pressure . . . 7
2.4 Wall Shear Stress . . . 8
2.5 Mechanotransduction and cell morphology . . . 8

3 Methods **9**
3.1 3D lumen fabrication . . . 9
3.1.1 Chip fabrication . . . 9
3.1.2 Surface activation . . . 9
3.1.3 Viscous finger patterning . . . 9
3.2 Lumen characterisation . . . 10
3.3 Connecting the microfluidics . . . 10
3.4 Flow analysis . . . 10
3.4.1 Video acquisition . . . 10
3.4.2 Data analysis . . . 11
3.5 Cell culture . . . 11
3.6 Cell seeding in three-dimensional collagen lumens . . . 11
3.7 Proof-of-principle flow experiment in the 3D-vessel-on-a-chip . . . 12
3.7.1 Flow application . . . 12
3.7.2 Immunohistochemistry and imaging . . . 12

4 Results **13**
4.1 Lumen creation and characteristics . . . 13
4.2 Flow analysis . . . 13
4.3 Cell culture and immunohistochemistry . . . 14

5 Discussion and Recommendations **17**

6 Conclusion and Future Outlook **20**

7 Acknowledgements **21**

8 Appendix **24**
8.1 Protocol: Applying flow in 3D vessel-on-a-chip systems . . . 24
8.1.1 Materials . . . 24
8.1.2 Procedure . . . 24
8.2 MATLAB scripts . . . 25
8.2.1 Lumen width analysis . . . 25
8.2.2 Flow profile plotting . . . 26
8.2.3 Video processing . . . 27
8.3 Data analysis immunohistochemistery in 3D vessel-on-a-chip systems . . . 29

1 Introduction

Microfluidic 'vessel-on-a-chip' systems are part of cutting edge research in the domain of 'organ-on-a-chip' engineering. The aim is to create an artificial blood vessel that closely mimics the physiological responses of a blood vessel *in vivo*. This is a key factor in drug research to cancer and numerous cardiovascular diseases.[1]

In research to these cardiovascular diseases there is a need for models utilizable for drug testing and investigation of the complex disease mechanisms. In this field most of the *in vitro* vessel model studies are based upon 2D cell cultures, such as monolayer studies, Transwell studies and pseudo-capillary cell culture studies. These models are common and convenient, but lacks important factors in the microenviroment of the cells.[1] Insufficient light is shed on factors such as stiffness, mechanical stimuli, complex blood vessel structure and fluid flow.[2] Therefore, the focus in studies using 2D vessel models lies on the cellular biology and molecular mechanisms instead of blood vessel function. In recent years, the interest in more complex 3D vessel models has significantly increased. Among various 3D vessel models is the 3D hydrogel-based vessel-on-chip. This model contains a microfluidic cylindrical lumen which allows for incorparating cells in the hydrogel matrix. This model is capable of exhibiting not only the basic cell biological and molecular properties of the cells present in the inner layer of the blood vessel, but also capturing the morphology and (patho)physiology of blood vessels in total.[1] Testing potential or newly developed therapeutic drugs is one of the fields on which these more advanced models will have a major impact.[1]

To achieve a realistic 3D hydrogel vessel-on-a-chip viscous finger patterning (VFP) shows promising results.[3] VFP is based on the principle that a fluid with a certain viscosity displaces another fluid with a higher viscosity, resulting in finger-like projection of the less viscous fluid.[4] Studying the flow and shear stress when using this manufacturing technique is important for creating accurate *in vitro* vessel models. Understanding the fluid dynamics inside the vessel makes it possible to predict and adapt the wall shear stress (WSS) on the endothelial cells lining the lumen wall and gain knowledge about the initiation and progression of certain vascular diseases.
In vivo fluid flow is induced by the heart that pumps blood through the vessels. This movement of fluid exerts a WSS and stretches the wall of the blood vessel. Endothelial cells can sense flow via mechanotransduction and regulate the vessel physiology accordingly. WSS plays a major role in for instance focal distribution of artherosclerotic lesions and endothelial homeostasis.[5]
3D hydrogel-based vessel-on-a-chips are increasingly utilised in several researches. However, no standardised protocol is present to allow the addition of flow in the lumen of the vessel at the AST research group. Such protocol will allow for a standardised method to set the flow for a desired shear stress. Furthermore, cross-comparison between researches will become easier.

In this assignment a protocol that enables users of 3D hydrogel-based microfluidic vessel-on-a-chip systems to introduce fluid flow to their experiments will be proposed and tested. To guarantee a suitable and workable protocol two experiments will be performed. Firstly, characteristics of the vessel lumen, such as diameter and straightness, were determined. Successively, the flow and WSS were determined inside the the vessel-on-a-chip system without cells to evaluate the assumptions made in flow and WSS calculations. Secondly, flow will be applied to the 3D hydrogel-based vessel-on-chip with induced pluripotent stem cell-derived endothelial cells (iPSC-ECs) lining the lumen wall to evaluate the morphology of the endothelial cells under a physiologically relevant flow rate.

2 Theory

To comprehend the methods and the generated result background information will be given about relevant topics. Firstly, characteristics of blood vessel present in the circulatory system will be described. Secondly, the used 3D hydrogel-based vessel-on-a-chip and theory about the fluid dynamics in the lumen is explained. Lastly, the cell behaviour under these flow conditions is discussed.

2.1 Blood Vessels *in vivo*

Almost all blood vessels are composed of three layers as illustrated in figure 1. The outer layer, *tunica externa*, mainly consists of collagen fibers. These fibers offer reinforcement and protection and give stability by anchoring to nearby structures. The middle layer, *tunica media*, consists of smooth muscle and elastic fibers. This layer can cause vasoconstriction and vasodilation regulating blood pressure and circulation. The inner layer, *tunica intima*, is the lining of the vessel containing endothelium. The endothelium is slick to reduce friction during transport of blood and very thin to allow efficient exchange between the blood and surrounding cells. Larger vessels(>10mm) also contain a subendothelial layer to support the endothelium.[8, 9] The average endothelial cell has a length of 20 to 40 μm, a width of 10 to 15μm and a height of 100 to 500 nm.[10] These cells physiologically experience a shear stress around 100 mPa to 600mPa in the venous system and 1 Pa to 7 Pa in the arterial system.[11]
Blood vessels are of utmost importance in gas and nutrient exchange as well as transporting other compounds. The vascular system is very complex, due to the wide extent of presence in the body as well as the various functions it has in different organs. This complexity makes the blood vessel a important factor in primarily vascular diseases and diseases that are directly or indirectly traced back to the dysfunction of the vascular system.[1]

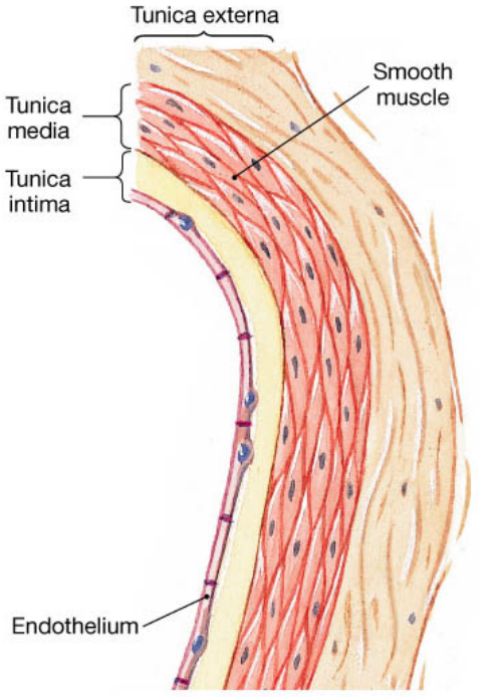

Figure 1: Overview of a venous vessel wall indicating the vessel layers and components.[6]

2.2 3D vessel-on-a-chip

To gain knowledge about the pathophysiology and physiology of the vascular system models of blood vessels are widely used. Most of them are relatively simple 2D models which provide knowledge about the cellular biology and complex molecular mechanisms. However, these models lack a dimensional element, which can lead to an inaccurate representation of the vascular physiology.[1] Therefore, there is a strong interest in models that represent the blood vessel including a 3D lumen. Great progress in the domain of organ-on-a-chip has made it possible to generate compact, dynamic and more complex *in vitro* 3D vessel-on-a-chips.[1]
The chip used in this study is made out of polydimethylsiloxane(PDMS).[12] This polymer is widely used in microfluidics because the low cost and and complex designs that can be created. Furthermore, optical transparency allows convenient monitoring and gas permeability allows transport studies and long term experiments.

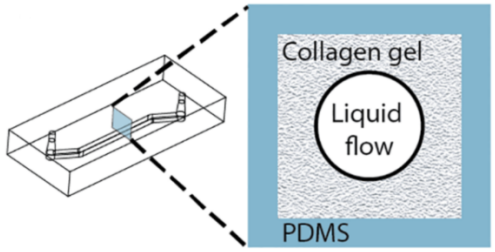

Figure 2: A top view and cross section of a 3D microfluidic vessel-on-a-chip.The 3D-vessel-on-a-chip consist of a PDMS channel that is filled with collagen. A lumen is created by the viscous finger patterning method. In this lumen cell can seeded an flow can be applied.[7]

PDMS is casted into a mould to create a chip with a rectangular cuboid channel. An inlet and outlet is punched to gain access to the channel. A PDMS coated glass slide is attached to the bulk material to obtain a closed channel system.[12] To facilitate covalent binding of collagen to the channel surface is activated.[13] After this, channel system is filled with collagen and a lumen is created using viscous finger patterning, further described in section 3.1.3. The result will be a collagen filled PDMS channel with an cylindrical lumen, as shown in figure 2. The obtained cylindrical lumen can be seeded with cells to complete the 3D vessel-on-a-chip.

2.3 Pressure-driven Flow

In order to be able to perform experiments with microfluidic systems, some type of fluid flow has to be initiated. When a pressure is applied at one of the openings of a tube, fluid moves from the higher to the lower pressure. This method is called pressure driven flow. First of all an overview of the characteristics of flow will be given in sections 2.3.1 and 2.3.2. After this, a few methods of application of flow will be discussed in sections 2.3.3 and 2.3.4.

2.3.1 Laminar and turbulent flow

There exist two types of flow behaviour: turbulent and laminar flow.[14] Turbulent flow encourages rapid mixing of fluids and thus is applied in micromixing systems. Laminar often used, because it enables precise calculations of the fluid behaviour and is very predictable. The type of flow is determined by the size of the channel, the viscosity and density of the fluid and the flow velocity. The type of flow is determined by the Reynolds number[15, 16, 17]:

$$Re = \frac{Inertial\,force}{Viscous\,force} = \frac{\rho u d}{\mu} \tag{1}$$

In this equation, ρ is the density of the fluid in $\frac{kg}{m^3}$, u is the linear flow velocity in $\frac{m}{s}$, d is the characteristic length of the channel perpendicular to the flow in m and μ is the viscosity in $Pa \cdot s$.
The Reynolds number is dimensionless. This is convenient for scaleable models, because systems with equal Re-numbers will behave in similar ways. A Reynolds number below 10 indicates a laminar flow. A Reynolds number larger than 2000 indicates a turbulent flow. In the intermediate regime, flow is mostly laminar but there is no guarantee. This also depends on the geometry of the vessel.[17] The blood flow in larger arteries is turbulent, while the flow in small vessels is mostly laminar. Alteration of the geometry of these vessels can occur, due to certain cardiovascular diseases. This also induces turbulent flow downstream from the irregularity in these vessels causing further vascular remodeling.

2.3.2 Flow profile

When a pressure gradient is applied over a vessel, the fluid in the tube will start to accelerate. This acceleration is opposed by frictional forces in he fluid. The quantity of this force depends among others on the viscosity of the fluid. On the walls of the vessel we can assume that the linear flow velocity is zero due to adhesion.[5] Towards the center of the vessel the linear flow velocity increases, because less frictional force from slower moving fluid is experienced further from the wall. This results in a parabolic flow pattern as shown in the fully developed region in figure 3. At the entrance region, the flow is not yet fully developed and has a less parabolic flow pattern. When assuming that the fluid is in steady state and compressible the flow velocity in a straight cylinder at fully developed flow can be calculated at a set distance from the wall by the Poiseuille flow equation[18]:

$$U(a) = -\frac{1}{4\mu L}(a^2 - r^2)\Delta P \tag{2}$$

In this equation, ΔP is the pressure drop in Pa, r is the vessel radius in m, L is the vessel length in m and a is the distance from the center of the vessel in m.

2.3.3 Active Pumping

Common techniques of active pumping are syringe pumping and pressurisation. A syringe pump applies the pressure needed to obtain a constant volumetric flow. This method is easy to set up and enable precise control over a wide range of flow rates. However, the pressure needed to apply high flow rates could exceed the limits of equipment in this method, which is disadvantageous. A second disadvantage is that a syringe pump has a slow response. Changes in flow can take some time and the flow rate can not be accurately known in these transient periods.[20]
Pressurisation uses a pump to apply a constant pressure over the system. This method is more responsive than syringe pumping and ensures pulseless flow. The biggest disadvantage of this setup is that the volumetric flow can not be known accurately without a flow sensor. These systems also have a higher cost and high pressures are not feasible. For both methods, the fluid dispensing is a limiting factor which can be problem in long lasting experiments.[20]

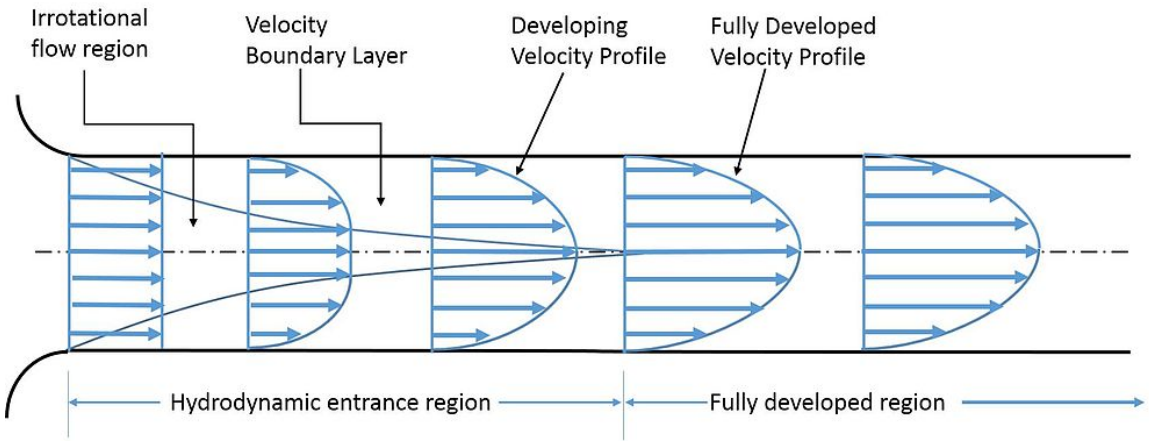

Figure 3: Visualisation of flow profiles over different regions in a cylindrical vessel. The blue arrows indicate velocity vectors. [19]

When setting the volumetric flow the pressure drop over a straight vessel can be estimated with the Hagen-Poiseuille equation[16]:

$$\Delta P = \frac{8\mu L Q}{\pi r^4} \tag{3}$$

In this equation μ is the viscosity in $Pa \cdot s$, L the length of the vessel in m, Q the flow rate in $\frac{m^3}{s}$ and r the radius of the vessel in m. The actual pressure drop in a vessel-on-a-chip system will slightly deviate from the calculated value due to imperfections in the vessel wall.

2.3.4 Fluid Pressure

Next to active pumping, another way of propelling fluid through a vessel is by applying a pressure difference generated by the fluid itself. Two methods of this are passive pumping and hydrostatic pressure. The principle of passive pumping is based on the difference in surface tension between a droplet at the inlet and outlet. A big droplet has a lower surface tension than the small droplet. Therefore, if a big and small droplet are pipetted on the in- and outlet of a channel, a flow will be generated towards the bigger droplet.[21] The pressure difference at an air/liquid interface can be estimated by the Young-Laplace equation[21]:

$$\Delta P = \frac{2\gamma}{R} \tag{4}$$

In this equation, P is the pressure in Pa, γ is the surface tension in $\frac{N}{m}$ and R is the radius of the droplet in m. The pressures of both droplets can be calculated to obtain a pressure difference between the two ports. However, the pressure difference that can be generated is very low due to the surface tension that will break if a droplet becomes to large.[21]

Hydrostatic pressure can be used to generate higher pressure differences. When using pipette tips, a pressure gradient is created by the gravitational pull on the fluid in the tip. This is produces a hydrostatic pressure difference. The fluid level is placed at a certain height above the microsystem and as such a pressure drop occurs. This pressure drop can be calculated by following equation[22]:

$$\Delta P = \rho g H \tag{5}$$

In this equation, ρ is the density of the fluid in $\frac{kg}{m^3}$, g is the acceleration due to gravity (9.81 $\frac{m}{s^2}$) and H is the height of the fluid level above the chip in m.
This method is very easy to implement. However, from the equation it can be deducted that the pressure drop is not constant over time. When fluid flows from the inlet to the outlet, the fluid levels and thus the hydrostatic pressure difference decreases. Therefore, the flow rate and wall shear stress is hard to control.[23]

2.4 Wall Shear Stress

The wall shear stress(WSS) in a vessel is the force exerted on the surface of the lumen tangent to the flow. A high flow rate is proportional to a high WSS and vice versa.[5] In circulation blood flow exerts a force on the vascular endothelium.
For a straight cylindrical channel the wall shear stress can be calculated according to equation 6. For this equation a few assumptions have to be made. The fluid inside the vessel has to be a Newtonian fluid, the vessel has to be cylindrical and the flow profile inside the vessel has to be parabolic and fully developed.[24, 5]

$$\tau = \frac{4Q\mu}{\pi r^3} \tag{6}$$

In this equation, τ is the shear stess in Pa, μ the viscosity in $Pa \cdot s$, Q the flow rate in $\frac{m^3}{s}$ and r the radius of the vessel in m.

In *vivo* WSS has an effect on the vessel wall diameter, while the wall diameter is regulated by the tension that is present on the wall. This hemodynamic factors are very important for the physiology of the vessel wall.[26]
The transduction of the shear stresses in the endothelium is a complex mechanism. The physical deformation of the endothelium is transmitted in the cell, which converts the stress in to chemical activity. The cytoskeleton of the endothelial cells is an important factor in this transduction.[27]

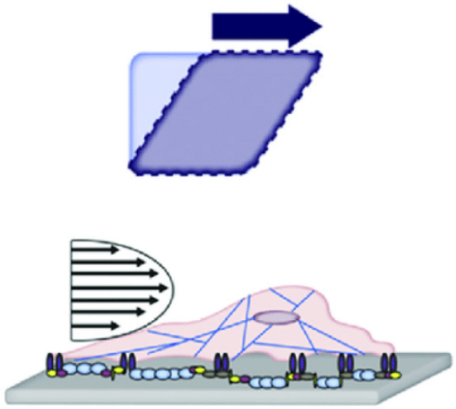

Figure 4: A simplified representation of the effects of shear stress on a cell. For both an idealized square(top) and a cell(bottom) the effect of the shear stress caused by a flow parallel to the channel wall is shown. [25]

2.5 Mechanotransduction and cell morphology

As stated in the previous section, WSS has a great influence on the morphology and cytoskeletal strucure of endothelial cells. When a flow is applied the cells tend to align with the flow direction. This means that the cell will elongate in the direction of the generated shear stress, as shown in figure 4. When under high WSS, the microfilaments of filamentous actin(F-actin) in the cell will predominantly lay parallel to the flow to oppose the forces exerted on the cytoskeleton. Under low WSS, the direction these filament will be evenly distributed over the cells periphery. The redistribution of these microfilaments increases the ability of the cell to adhere to the ECM as to maintain the monolayer integrity. The intracellular cytoskeleton is connected to the ECM via integrins at focal adhesion sites. These sites are present at the ends of actin containing microfilament bundles where the cell meets the ECM. Cellular signaling can cause the intracellular binding of talin to integrin initiating the extracellular binding to the ECM and the intracellular binding of vinculin and actin. Vinculin and talin are both focal adhesion associated cytoplasmic proteins that are present in the focal adhesion sites. Tension causes talin to unfold, which makes binding sites for vinculin available. This results in additional binding of actin filaments and development of the actin network as a response to WSS.[28, 29] In the junctional mechanosensory system between the endothelial cells vascular endothelial cadherin (VE-cadherin) is an important adherence protein.[30]

3 Methods

3.1 3D lumen fabrication

The first step in creating a vessel-on-a-chip model is producing the foundation for the endothelial cells to be seeded on. Firstly, a PDMS chip is fabricated as base to produce a collagen lumen in. Secondly, before collagen can bind to the PDMS surface activation has to be performed. Lastly, a lumen can be produced inside a collagen matrix with the viscous finger patterning method.

3.1.1 Chip fabrication

Polydimethylsiloxane (PDMS, SYLGARD 184, Dow Corning) silicone elastomere base was mixed 10:1 with silicone elastomere curing agent. Air bubbles were removed by degassing the PDMS in a dessicator. The degassed PDMS is transfered to a clean mould. The channels in this mould were 500μm high 500μm wide and 1 cm long, as shown in figure 5. To remove leftover air, especially near the channels, the PDMS is degassed once more in the desiccator. Next, the mould was incubated overnight at 65°C. The chips were cut to have six channels each. Inlets and outlets were punctured using a 1mm diameter Biopsy punch (Robbins instruments). The cut and punctured chips were covered with scotch tape to protect them from dust and debris. After this, glass coverslides were spincoated(SPS Spin 150 Spin Coater, 5s at 500rpm followed by 30s at 1500rpm) with PDMS. These were incubated overnight at 65°C.
The cured PDMS chips and cover slides were plasma treated (40s, 50W and 50kHz at 0.5 torr) in a plasma system (Femto science CUTE). The two pieces were bonded after plasma oxidation through assembling and applying pressure for approximately 15 seconds.

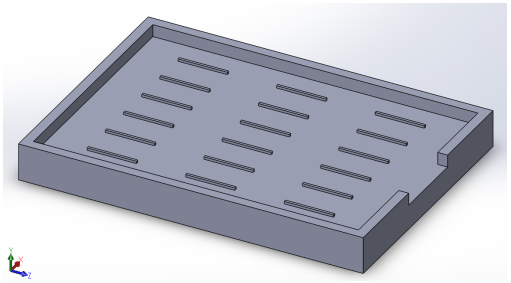

Figure 5: The used mould for producing microfluidic chips visualised in SolidWorks. 18 channels can be produced with this mould. The channel dimensions are 500μm $\times$500μm $\times$1$cm[w \times h \times l]$

3.1.2 Surface activation

3% (v/v) (3-aminopropyl)-triethoxysilane (APTES, Sigma-Aldrich) in milliQ was into the channels on the chip until a droplet was formed at the outlet. APTES has to be handled under nitrogen flow, because it is very reactive to the water in the air. After 5 minutes the APTES was removed by rinsing the channels with 100% ethanol. The chips were placed upside-down in a petridish with the bottom covered with ethanol for 2 minutes. The channels were rinsed again with 100% ethanol and dried with a nitrogen gun.
After this, 10% (v/v) glutaraldehyde (GA, Sigma-Aldrich) in milliQ was pipetted in the channels until a droplet is formed at the outlet and left for 5 minutes. This process was done one chip at a time, because after removing the APTES the surface is very reactive and there has to be acted quickly. The GA was removed by rinsing the channels with demi-water and incubating the chips for 20 minutes at RT. After this, the channels were rinsed again with demi-water followed with 100% ethanol and dried using the nitrogen gun.

3.1.3 Viscous finger patterning

Surface activated chips were incubated at 37°C for 2 to 4 hours. A collagen solution was prepared including rat tail collagen I(9.1mg/mL, Corning), 1M sodium hydroxide(NaOH,Sigma-Aldrich), milliQ and Phosphate Buffered Saline 10X(PBS, Gibco). All were kept on ice to reduce the cross-linking of the collagen before adding it to the channels.
To produce 50 lumens in the chips 167μL milliQ, 50μL 10X PBS and 6.32μL NaOH were pipetted into one eppendorf for the stock solution. In another eppendorf 275μL collagen was pipetted. The stock solution was pipetted in the collagen solution in a swirling motion. This collagen solution is vortexed and centrifuged to mix and remove bubbles. The final 5mg/mL collagen solution was kept on ice and used within 1 hour.
10μL of solution was pipetted into the channel until a droplet is formed at the outlet. Another pipette tip with 25 μL of PBS is inserted at the outlet with the droplet. The pipette tip is ejected from the pipette without pushing the fluid inside the channel. At the inlet the surface tension was broken and an empty pipette tip inserted. viscous finger patterning can be confirmed by a rising fluid level in the empty tip. A schematic representation of this procedure is shown in figure 6 The chips were placed in the incubator at 37°C to cross-link the patterned collagen.

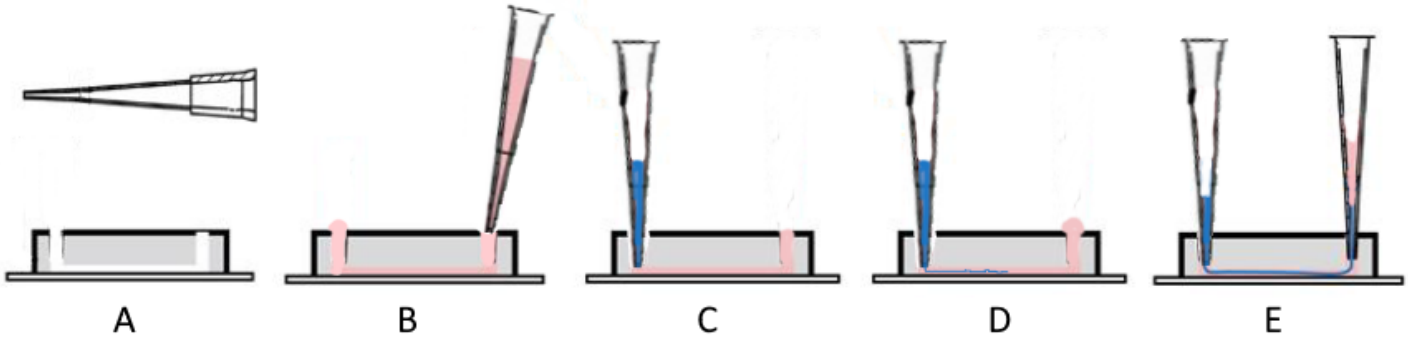

Figure 6: Schematic overview of the viscous finger patterning technique. A surface treated chip is placed onto a level surface.(A) Collagen, shown in pink, is pipetted into the channel until a droplet forms at the outlet.(B) Then a pipette tip with PBS, shown in blue, is placed into the outlet.(C) The PBS will creep through the collagen.(D) When the droplet at the inlet starts increasing in size, a empty pipette tip is placed into the inlet. This pipette tip will start to fill up.(E)

3.2 Lumen characterisation

The lumens were imaged with the Nikon TE-DH100W. The width of the lumens is determined with MATLAB. The used script is shown in the appendix, section 8.2.1. In this script a straight line can be drawn over one of the walls and a point on the other wall can be selected. To obtain the channel width the perpendicular distance between these two is calculated.

3.3 Connecting the microfluidics

The syringe pump was connected to the chips according to the protocol in the appendix, section 8.1. Microfluidic tubing was connected to a 5mL syringe (BD Plastipak) and a blunt needle. Both the tubing and blunt needle had an inner diameter of 1mm. After disinfecting the syringe it was a quarter filled with PBS to reduce pulsatile flow behaviour, due to the compressibility of air left in the syringe. The syringe was mounted onto the syringe pump. One of the pipette tips in the chip was removed and the blunt needle was inserted into the inlet. The other pipette tip acts as a reservoir.

3.4 Flow analysis

The flow will be visualised by supplementing PBS with beads and pumping this through the lumen. Firstly, a video was be recorded from a region in the channel. Secondly, the bead velocity in the video's were analysed to produce a flow profile. Shear stress on the channel wall was determined using this flow profile.

3.4.1 Video acquisition

A chip was fixed to a petridish with scotch tape. This petridish was mounted under an EVOS FL imaging system with camera and fixed to the stage of the microscope to avoid motion while imaging. A video (1024x768, 30 frames per second) of the microscopy was obtained by recording the screen of the microscope with a HDMI cloner box. One of the microfluidic channel was connected to the syringe pump. PBS was supplemented with beads(Polybead microspheres 10.00μm, Polyscience) to obtain a suspension with a concentration of $1.365 \cdot 10^6$ beads/mL. The video was recorded at the middle of the channel at flowrates of 5μL/min, 10μL/min and 15 μL/min. Before every recording the flow was allowed to settle for 60 seconds.

3.4.2 Data analysis

To distinguish the non-moving beads from moving beads some video processing was done. In MATLAB a foreground detector was used to determine if pixels in the video are part of the background or foreground. The background is subtracted to obtain a gray-scale video in which only the foreground, thus moving, beads are visible. One video frame when using this technique is shown in figure 7. The MATLAB script used for the video processing is attached in the appendix, section 8. The velocity of a bead was determined by taking two consecutive frames and manually counting the pixels a bead has travelled. This was done for 15 beads per channel at two moments in the video. Shear stress was calculated using the maximum velocity of the beads and the diameter of the channel. Equation 6 was used for estimating the shear stress on the channel wall assuming the viscosity of the PBS buffer at 25°C is 0.0009 Pa·s.[31]

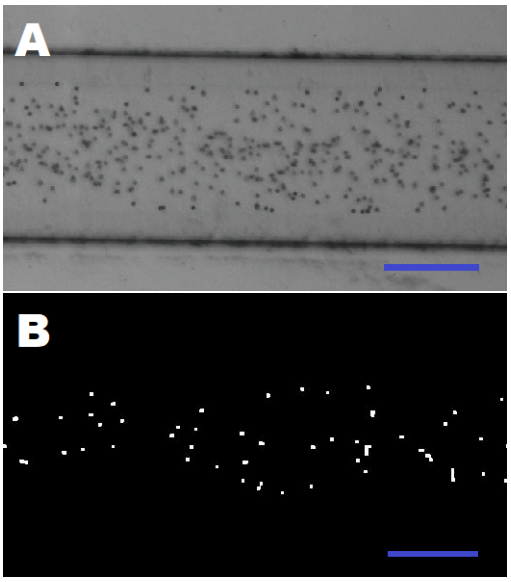

Figure 7: Object tracking is applied to the acquired video to distinguish all moving beads from stationary beads. In (A) a frame from the original video is shown and in (B) the processed image is shown. The scale-bars represent 200μm.

3.5 Cell culture

Firstly, 4 T25 flasks were coated with 3.5mL 0.1%(wt/v) gelatin(Porcine Skin gelatin, Sigma Aldrich) for 1 hour, after which the bulk gelatin is aspirated. Induced pluripotent stem cell–derived endothelial cells(iPSC-ECs, diff. 10, ±500k) were thawed in a 37°C water bath. After disinfecting the cell eppendorf with 70% ethanol, the cells were suspended in 9 mL basal Human Endothelial Serum Free Medium(EC-SFM, Thermo Fisher). This suspension was centrifuged(300g, 3 min) to obtain a cell pallet. The supernatant was aspirated. The cell pallet was resuspended in 22mL EC-SFM full medium(1%(v/v) platelet-poor-derived serum(Biomedical Technologies), 30ng/mL Vascular endothelial growth factor(VEGF, Miltenyi Biotec),20ng/mL basic fibroblast growth factor(bFGF, Miltenyi Biotec)). The T25 flasks were each filled 5.5mL cell suspension and incubated for 3 days.

3.6 Cell seeding in three-dimensional collagen lumens

After culturing the cells for 3 days, the medium was aspirated from 2 flasks. The cells were washed with 2mL Dulbecco's phosphate-buffered saline(DPBS). 1mL trypsin/EDTA(0.5%, Thermo Fisher) was added and the flasks were incubated for 3 minutes at 37°C. Endothelial cell growth medium 2(ECGM-2, Promocell) complemented with penicillin/streptomyocin at 10U/mL,10 μg/mL was added to inactivate the trypsin, the cells were harvested and transfered to a 15mL tube and centrifuged(300g, 3 min). After centrifugation, the supernatant was aspirated and the cells were resuspended in 100μL ECGM-2. After this, cells were counted and diluted in ECGM-2 to have a cell concentration of $7.5 \cdot 10^6$ cells/mL.
5μL of the suspension was injected into the lumen with a gel loader tip. After this, the chip is incubated upside down for 1 hour to coat the top of the lumen. The protocol was repeated with the remaining flasks and right side up incubation to coat the bottom of the lumen. The chip was finalized by flushing all non-attached cells out of the lumen and refreshing the medium. This was done by aspirating the medium from one of the pipettes until the fluid level in both pipettes is low. This is done without letting air inside the channel. After this 150μL of ECGM-2 was added to the other pipette and the chips were placed on a rocker device, consisting of a platform at 60 degree which tilts every 30 seconds.

3.7 Proof-of-principle flow experiment in the 3D-vessel-on-a-chip

3.7.1 Flow application

The protocol used in section 3.3 is limited to a reservoir volume of 200μL, so modifications had to be made to allow for bigger volumes. Per channel a 50 mL tube was prepared by drilling 2 1mm holes in the cap of the tube. In one of the holes a blunt needle was inserted and the other was left open to let air escape the tube. Microfluidic tubing was disinfected with 70% ethanol and cut to the correct length. Per 50mL tube a piece of tubing was connected to the blunt needle at the underside of the cap and suspended around 1mm above the bottom of the tube. Another piece of tubing was cut to connect the blunt needle at the top of the cap to the inlet of the chip. A blunt needle was used in the tubing-chip connection. Lastly, a piece of tubing is cut to connect the syringe to the outlet of the chip. A blunt needle with a luer lock was attached to a 60 mL syringe(BD plastipak). One end of the tubing was slided over this needle. At the other and a blunt needle is inserted in the tubing. After this the tubing and tubes were disinfected by flushing the syringe-tubing and tube-tubing combinations with 70% ethanol. When the ethanol was evaporated the tube was filled with ECGM-2 medium. One of the pipette tips was removed out of the inlets. To avoid getting air bubbles into the channel a syringe with blunt needle luer lock was placed in the open hole in the cap and used to push medium through the tubing to the end of the blunt needle by pressurizing the air in the tube. When droplet formed at the needle it was inserted into the inlet. At the outlet the pipette was removed and the blunt needle from the syringe inserted. The obtained setup is shown in figure 8. The chips and the tubes with medium were put in the incubator at 37 °C. The tubing from the syringe was led through the outlet port of the incubator to the syringe pump.

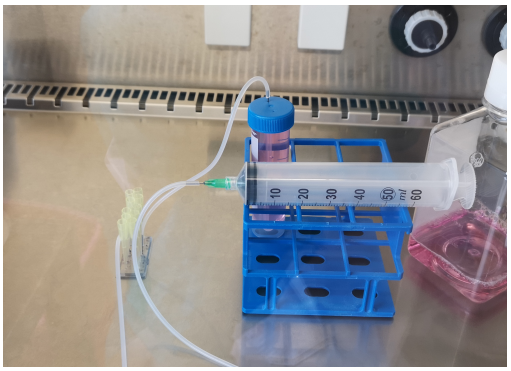

Figure 8: The used setup before placing the chip and medium in the incubator. The tube with medium is connected to the chip with two microfluidic tubes and a blunt needle through the cap of the tube. The syringe in connected to tubing with a blunt needle attached to a luer lock. The other side of the tubing is attached to a blunt needle and inserted in the inlet of the chip.

The syringe pump was set at 1.8mL/min to generate an expected WSS in the range of 6.3 Pa in a channel with a diameter of 350μm. This flow rate value was tested because this produces a WSS that lays within the range of arterial shear stresses mentioned in section 2.1. A study by Cucina et al. showed that endothelial cells showed morphological changes after being subjected to a shear stress of 600mPa for 24 hours.[32] A study by Silvani et al. showed that endothelial cells will have a slight orientation bias after being subjected to a shear stress of 800mPa for 4 hours with a major bias after 48 hours.[33] To increase the probability of observing morphological changes within an experiment time of 6 hours a high physiological WSS was applied. To avoid using 648mL of medium per chip over the course of 6 hours, the 60mL syringes were emptied back into the tubes every 25 minutes. This was done 11 times over a timespan of 6 hours. During this procedure the microfluidic tubing to the syringe was first closed of by bending the tubing to avoid letting air inside the system. The syringe was removed from the luer lock and emptied in the tube. The cap of the tube was removed without taking the tubing at the underside of the cap out of the medium. Two seeded chips that were not exposed to shear stress were used as control group.

3.7.2 Immunohistochemistry and imaging

Medium was removed from the lumen and a pipette with 50μL 4%(wt/v) formaldehyde was inserted in the inlet. When a meniscus formed at the outlet a pipette with 50μL 4%(wt/v) formaldehyde was inserted in the outlet and the chip was incubated for 15 min at RT. After fixation, permeabilisation and blocking buffer (0.1% Triton X-100 in 1%(wt/v) BSA in PBS) was incubated for 1 hour at RT. In each channel 50μL of VE-cadherin primary antibody solution, containing 5μg/mL Goat Anti-Human VE-Cadherin(RD Systems) in PBS, was added. After incubation overnight at 37°C, the staining solution was aspirated and washed with PBS. After this 50μL a secondary antibody staining solution, containing 10μg/mL Donkey anti-Goat IgG Cross-Adsorbed Secondary Antibody Alexa Fluor 546(Thermo Fisher), 12.5μg/mL DAPI(Thermo Fisher) and 4 drops/mL ActinGreen(Invitrogen), was pipetted into the channels and incubated for 4 hours at RT. The staining solution was aspirated and the channels were washed with PBS. The chips were stored dark before imaging to avoid photobleaching. Imaging was performed with a confocal microscope.

4 Results

The main aim of this study was to produce a workable and suitable protocol for the application of flow inside a 3D hydrogel based vessel-on-a-chip. To test the protocol two experiments have been performed. Before the experiments the lumens created inside the chips were characterized. Firstly, a flow analysis has been done to validate the flow profile when applying low flow rates. Secondly, cells have been cultured and exposed to a physiologically relevant shear stress to analyse the cell morphology.

4.1 Lumen creation and characteristics

Before a lumen could be created inside chip, the chip itself was made. This was done according to the method in sections 3.1.1 and 3.1.2. For the flow analysis total 72 chips were used VFP according to the method described in section 3.1.3. From seven chips it could be confirmed that they had a very straight lumen. Two of these chips will be elaborated on in this section. The completed VFP chips were imaged. Using the method discussed in section 3.2 the width of the lumens shown in figures 10a and 10b were found to be 355.1 and 375.5 μm respectively.
In a lot of channels, no lumen was visible under the microscope. Rising fluid in the pipette is a visual sign that the PBS has pushed some collagen out of the channel. In some chips no lumen was produced, because no fluid was in the pipette. In other chips, there was fluid in the pipette when there was no lumen visible under the microscope, as shown in figure 9.

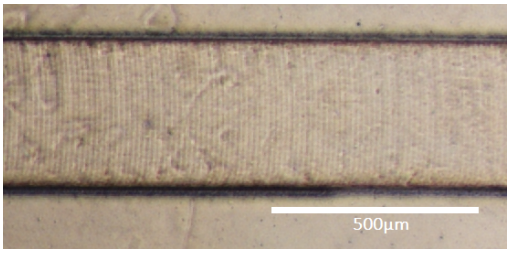

Figure 9: Channel in which no clear lumen is visible, even tough the fluid level in the pipette had risen.

4.2 Flow analysis

Application of technology in research, such as shear stress analysis, is further explored by determining the flow profile in the lumen. The velocity of beads for flow speeds of 5, 10 and 15 $\mu L/min$ were manually determined for the channels shown in figures 10a and 10b. The flow profiles of these channels are visualised in figures 10c-10h. For each flow rate a parabola could be reconstructed from the measured bead velocities. However, for the channel in figure 10a, the measured bead velocities are lower than the expected velocity in a straight cylindrical vessel. At 5 $\mu L/min$ this effect is more noticeable than at 10 $\mu L/min$. This effect is least noticeable at the highest flow rate, 15 $\mu L/min$. The channel in figure 10b shows a measured flow pattern that is close to the calculated flow pattern. However, both channels show large deviations in the bead velocity at comparable width.
From the average bead velocity, half the peak velocity, the measured flow rate was determined. These values are presented in table 1. The measure flow rates and the diameter of the channels, determined in section 4.1, were used to calculate the average WSS in the channels.

Table 1: Obtained data from the flow profile analysis

Lumen diameter (μm)	**Set flow rate (μL/min)**	**Measured fluid peak velocity (μm/s)**	**Measured flow rate (μL/min)**	**Shear stress (mPa)**
355.1	5	1063	3.16	10
	10	2289	6.80	23
	15	4169	12.39	42
375.5	5	1471	4.85	14
	10	2943	9.51	27
	15	4905	16.56	47

4.3 Cell culture and immunohistochemistry

The protocol presented in section 3.7.1 allows the application of high physiologically relevant flow rates in 3D hydrogel-based vessel-on-chips with endothelial cells lining the lumen wall. Here, a flow rate of 1.8 mL/min was applied to generate a WSS of 4.1 Pa (figure 11, middle column, 402.7μm lumen diameter) and 6.0 Pa (figure 11, right column, 356.8μm lumen diameter). This mimicks the WSS on the endothelial cells *in vivo* in the arterial system.
The endothelial cells in the control group (figure 11, left column) with no WSS applied appeared to have no directionality. The VE-cadherin proteins, stained with Alexa Fluor 546 and shown in figure 11j, form an irregular network at the periphery of the cells. Next to this, after staining with ActinGreen that specifically binds to F-actin, no orientation bias could be observed in the F-actin shown in figure 11g. The nuclei of the endothelial cells, stained with DAPI and shown in figure 11d, are mostly elliptically shaped and randomly oriented.
After 6 hours of WSS, the cells were observed to be elongated in the direction of the flow. This is shown by the VE-cadherin proteins, shown in figures 11k and 11l, which outline the elongated cells. In figures 11g and 11h, it can be observed that the F-actin is oriented more in the direction of the flow. The nuclei in figures 11e and 11f are similarly shaped as the nuclei from the control group. A difference can be observed regarding the orientation. The nuclei of the cells subjected to WSS seem to be positioned in the direction of the flow.
In the control group the endothelial cells were found to be evenly distributed over the lumen wall. The monolayer was mostly confluent, but some small gaps could be observed. In both lumens that were subjected to flow, big gaps were found. The locations where cells were present are mostly confluent. In other locations patches of cells seem to be missing.
In figures 11m, 11n and 11o a cross-sectional view is given of the seeded collagen lumens. None of these cross-sections are perfectly circular. The cross-section in figure 11m has a teardrop shape, the cross-section in figure 11n seems to be more square and the cross-section in figure 11o is elliptically shaped.

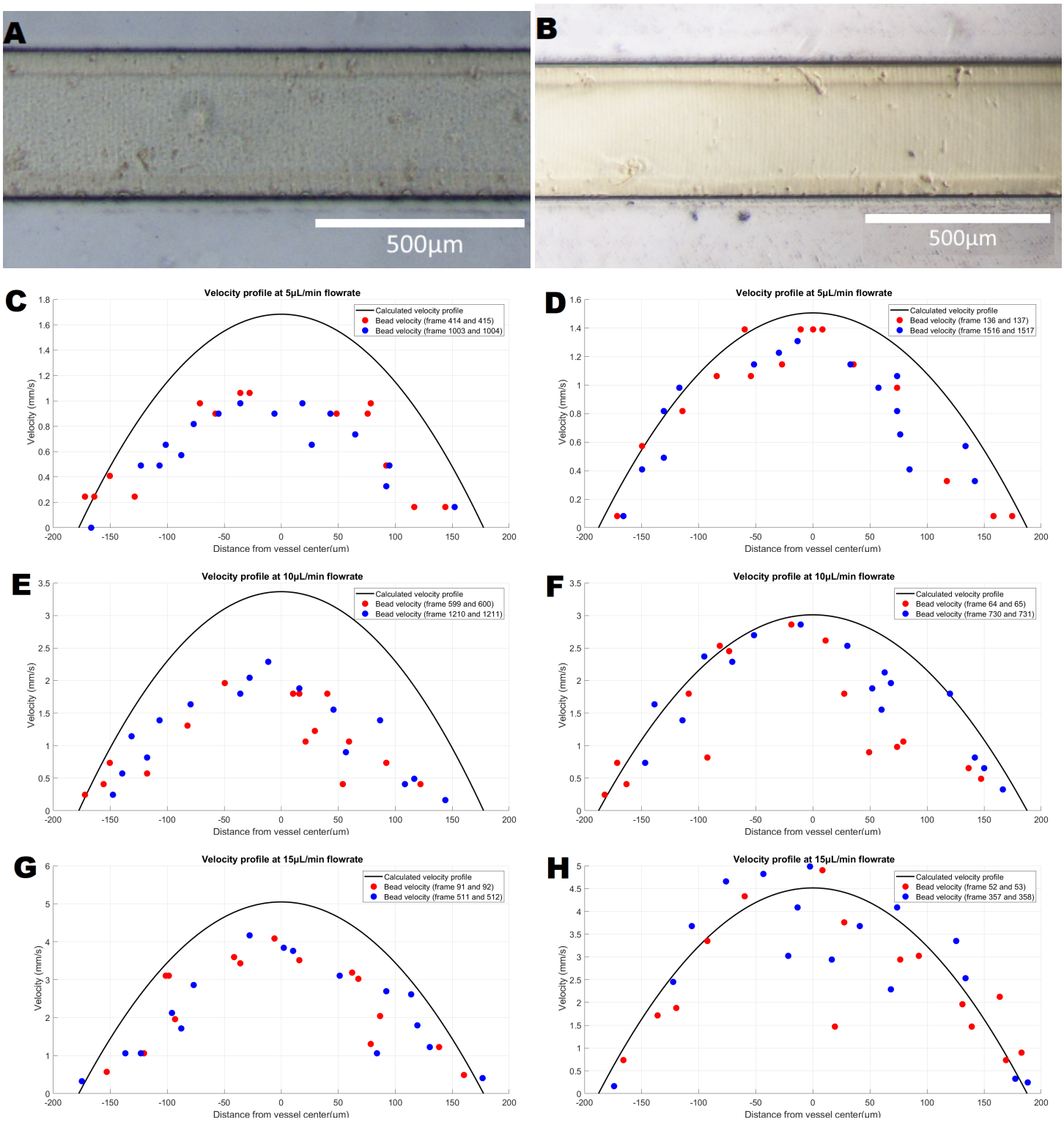

Figure 10: Analysis of the flow profiles. (A) and (B) Viscous finger patterned lumens imaged in the middle of the channel. These lumens were used for the flow experiments presented in section 4.2. The width of the lumens are (A): 355.1μm and (B): 375.5μm. (C),(E) and (G) The ideal flow profile and the flow profile reconstructed from bead velocities plotted over the width of the channel for the channel shown in (A). The profiles are shown for three flow rates: 5, 10 and 15 μL/min, respectively. (D),(F) and (H) The ideal flow profile and the flow profile reconstructed from bead velocities plotted over the width of the channel for the channel shown in (B).

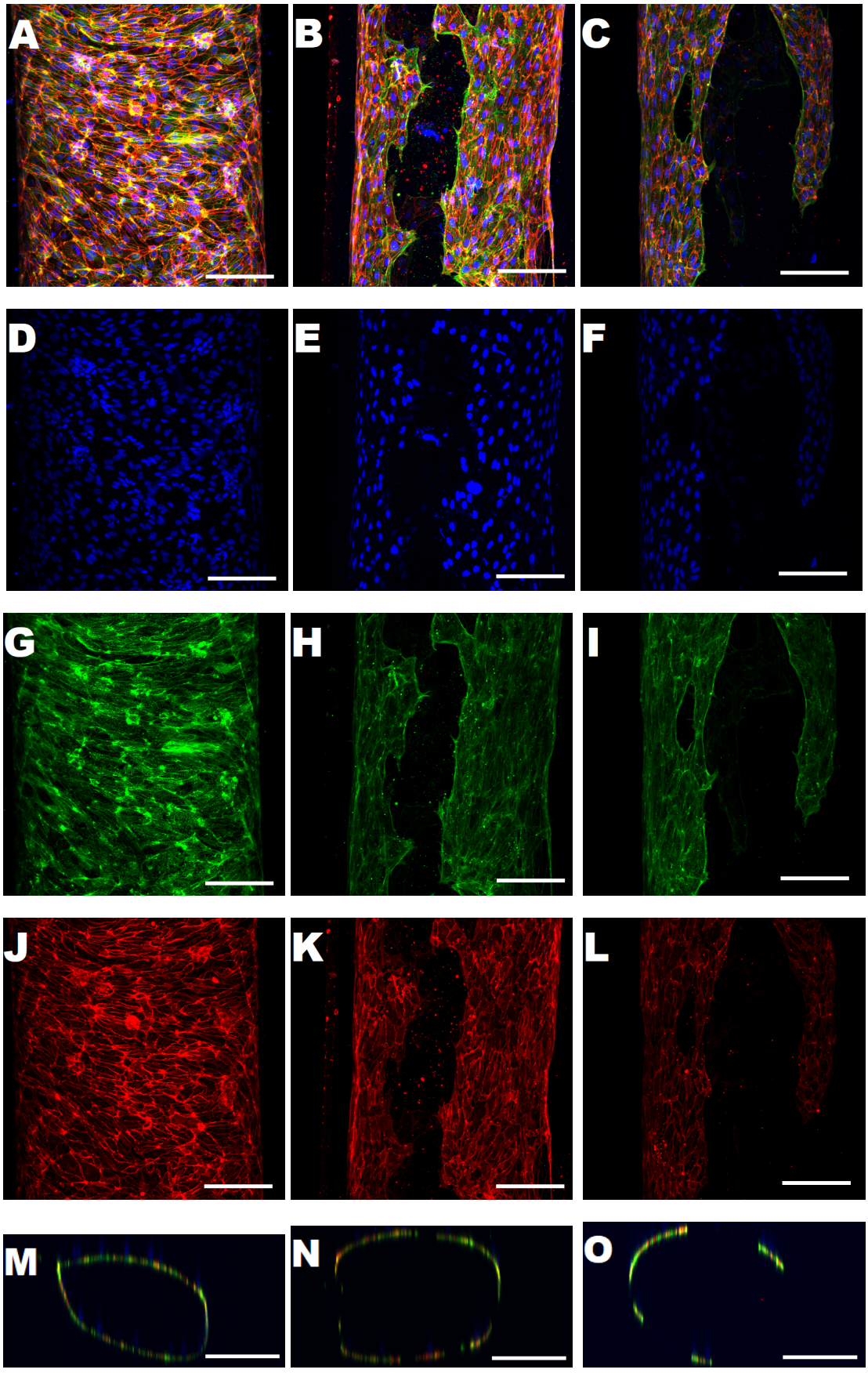

Figure 11: Cell morphology and channel geometry visualised using immunofluorescence and a confocal microscopy. (A), (D), (G), (J) and (M) show representative regions from the control lumens that were not exposed to WSS. (B), (E), (H), (K) and (N) show regions from channel 1 that was exposed to 4.1 Pa WSS. (C), (F), (I), (L) and (O) show regions from channel 2 that was exposed to 6.0 Pa WSS. (D-F) visualizes nuclei in blue, (G-I) filamentous actin in green, and (J-L) VE-cadherin in red and (A-C) a merged image of these stainings. (M-O) shows a cross-sectional view of each lumen respectively. Scalebars in panels (A-L) represent 200μm and in (M-O) 100μm.

5 Discussion and Recommendations

To assess and test protocols for flow and shear stress applications two experiments have been conducted. One the experiments focused on the flow profile of the fluid in the lumen, while the other experiment looked into the cell morphology of endothelial cells under a physiologically relevant WSS.

Before these experiments could be conducted, a microfluidic device had to be produced. In the production of the chips no complications occurred, but there are some point of attention. Degassing the PDMS in the mould is a crucial step to avoid bubbles near the channels, while these will disturb the flow inside the channel. When coating the cover slides, addition of to much PDMS will lead to coverage on the bottom of the slide. This causes the slide to stick to the surface it has baked on, which makes it hard to remove without breaking the slide. Channels with a square cross section where used for the VFP protocol. The accuracy of the manufacturing technique for the PDMS casting was not evaluated in this study. Because the exact dimensions of the moulds are not exactly known due to the resolution of the milling machine, the dimensions of the casted chips could deviate slightly.

Surface treating the microfluidic channels with APTES and GA is very effective. However, this method has intermediate steps that are time consuming, which causes the process to take approximately one hour. These intermediate steps increases the chance of human errors, which when accumulated can lead to inconsistencies between batches. APTES and GA are hazardous toxic chemicals and generate chemical waste. Therefore, it is preferential to use a more enviromentally safe and simple technique. An alternative is polydopamine, which is widely utilized and does not have the drawbacks of APTES in combination with GA.[34]

After surface activation, collagen lumens were produced in the surface activated chips using viscous finger patterning(VFP). This method had a low succes rate. The protocol used is prone to human errors and the lumen outcome is highly dependant on factors such as the fluid velocity through the collagen while patterning and the collagen viscosity. Pipetting a homogeneous collagen solution is therefore crucial to obtain similar results between batches, while the collagen viscosity is dependant on the concentration.[35] 9.1 mg/mL rat tail collagen stock solution was used. The collagen is very viscous and therefore adhered to the pipette tips. There not all collagen ended up in the collagen solution, which causes deviations between batches. To improve the reproducibility of VFP in further research the collagen could be quantified in weight and diluted accordingly.
Collagen solution was made for 50 lumens per batch. It was observed that the collagen starts to cross-link over time, even though the vial with the solution is kept on ice. Smaller batches should be produced and used directly to avoid pipetting cross-linked, more viscous, collagen inside the channels. When using collagen with a to heightened viscosity two observations could be made. In some cases a rising fluid level in the pipette could be observed, while in other cases the PBS did not flow through the channel. In both situations no lumen could be observed under the microscope. In the first case the PBS pushed the whole bulk of collagen out of the channel. In the second case the collagen was to viscous for the PBS to travel through.
Another method that is utilized to create a lumen is using a PDMS rod as placeholder for the lumen. Collagen is added to the chip around rod with the prefered lumen dimensions, that is removed after cross-linking of the collagen. This method has some advantages, such as enhanced control over lumen dimensions and the elimination of thermal polymerization issues present in the VFP method.[36] When characterising the lumen width the geometry of the lumen cross section was not taken into consideration. When calculating the flow rate and shear stress in section 4.2 the width of the is taken as input for the channel diameter. This is not representative while we do not know the geometry and average diameter of the channel cross section. In research by de Graaf et al. two-photon second harmonic generation (2P-SHG) with a Leica SP5 confocal microscope is used obtain a Z-stack 3D image of the channel. This imaging technique enables diameter analysis over the total length of the channel.[3]

On three chips of which a straight lumen was visible under the microscope the flow experiment was conducted. Firstly, the chip was connected to a syringe pump according to the protocol in the appendix, section 8.1. This protocol was effective at implementing flow inside a lumen without letting air inside the channel. However, one major drawback of this method, using pipette tips, is the volume limitation of 200μL. This is problematic for long lasting experiments or applying higher flow rates. In section 3.7.1 a method is described to connect reservoirs with a larger volume. This method can be easily adapted and scaled for specific experiments by interchanging the tubes and syringes. However, in cell experiments using large quantities of medium is not desirable. In the cell experiment presented in this research the medium was reused each

25 minutes. This is very labour intensive and a two person job, while the actions have to be performed in- and outside the incubator simultaneously. Therefore, in high volume cell experiments an alternative is desirable. A system that allows for recirculation of the medium is a peristaltic pump. These systems are easy to set up and are able to redispense the same sample infinitely. However, these kind of pumping systems do not allow as precise flow control as syringe pumps and might cause strong pulsations at lower flow rates. Furthermore, they generate vibrations and noise and require for more frequent replacement of tubing.[37]

In the flow profile experiment a two-dimensional velocity measurement has been performed on the beads. It has to be taken in consideration that the produced dimensional element and the beads were not all measured in one plane. This can lead to lower bead velocities than expected. For the analysis of the videos a MATLAB script has been used to distinguish the stationary beads from moving beads. This action had to be performed due to the interactions the beads have with the collagen wall. Some beads adhere to the wall, making manual velocity determination for the moving beads impossible. The manual determination of the bead velocity with video processing is still a labour intensive process. An alternative for this is an object detection MATLAB script that can calculate the bead velocity between two frames for every moving bead on screen. This has not been implemented in this study due to time limitations. When working with such scripts, it has to be taken in consideration that in the video the contrast between the beads and background has to be as high as possible. On three channels a flow profile experiment was performed, but from one of the videos the beads could not be properly detected by the script.

The calculation of the WSS is based on the Poiseuille law resulting in equations 3 and 6. These formula's are based on some assumptions. Firstly, the flow has to be laminar and fully developed.[5] Assuming the width of the channel in figure 10b the flow will become fully turbulent (Re>2000) at a flow rate of 29.9 mL/min. The flow is fully laminar(Re<10) at a flow rate lower than 149.3μL/min. According to the theory in section 2.3.1, this indicates that the flow is fully laminar in the vessel for the flow profile experiment. However, it has to be taken in consideration that slight imperfections and deformations in the lumen surface can produce alteration in the flow and initiate turbulence. In the cell experiment laminar flow can not be guaranteed, because the Reynolds number lies in the intermediate region. The flow has to have passed the hydrodynamic entrance length in the vessel to be fully developed. This entry length in laminar flow can be calculated by: $L_h = 0.05 \cdot R_e \cdot d$, with L_h the entry length and d the channel diameter.[38] For the channel that was used in the flow analysis this results in a hydrodynamic entry length of 0.39mm at a flow rate of 15μL/min. The flow profile analysis is performed further from the inlet. Thus, both assumptions were satisfied.
Secondly, the vessel has to be cylindical. As mentioned earlier, it could not be confirmed that the used lumens had a circular cross-section. Due to the high possibility of an alternatively shaped cross-section, as shown in section 4.3, the accuracy of the calculations could not be verified.[5]
Lastly, the lumen wall has to be rigid.[5] Application of flow inside a vessel-on-a-chip generates a transmural pressure. When this transmural pressure is significantly high, the collagen might deform and alter the channel dimension. Further research should be done to determine if this is a factor at physiological flow rates.
Comparable research to flow and WSS in vessel-on-a-chip systems has been performed by De Graaf et al.[3] The parabolic flow pattern obtained in that research does match the pattern in the performed experiment. However, the shear stress values deviated from the results found in section 4.2. After e-mail correspondence with the author it became clear that in equation 6 the π was forgotten when calculating the shear stress. When dividing the shear stress values from the research by de Graaf et al. by π the values correspond to the values obtained in this research.

The way endothelial cells respond to mechanical cues, such as WSS, is of great significance in the physiology of blood vessels, while this is often altered during disease progression. In this research it was observed that at physiologically high WSS endothelial cells will orient themselves in the direction of the flow. Some of these cells detached from the collagen lumen. The collagen lumens stayed mostly intact. However, near the inlet of the channel some detachment of the collagen from the PDMS could be observed. Detachment of cells or the collagen lumen can disturb the flow inside the channel, altering the WSS.

Assessment of the endothelial layer inside a vessel-on-a-chip is relevant in research to diseases or medicine. As described in section 2.5, endothelial markers can be used to assess the coverage and cell morphology of the endothelial cells. The permeability of the endothelial layer can be assessed by a permeability assay. This technique uses fluorescein isothiocyanate labelled (FITC) dextran to measure the permeation through the monolayer.[39]

Due to a shortage in time and lab spaces during the COVID-19 pandemic no in depth analysis could have been performed on 3D vessel-on-a-chips. An alternative for this was reviewing and analysing data generated earlier by Jim Koldenhof. Quantification of the immunohistochemistry images was performed in Cellprofiler software, but validity of the acquired value was a problem and lead to complications. When the images were assessed by eye, the obtained data from the Cellprofiler software did not match the staining observed in the image. An overview of this analysis is shown in the appendix, section 8.3.

6 Conclusion and Future Outlook

The main goal of this research was to assess the protocols for flow and shear stress applications. Firstly, a protocol was tested for a flow profile experiment. This protocol was suitable for a experiment using volumes lower than 200μL. From the flow profile experiment, it was observed that the produced 3D hydrogel based vessel-on-a-chip systems varied in dimensions and geometry, making exact WSS calculation a difficult procedure. However, a parabolic flow profile could be observed. Secondly, the protocol was adapted to be utilized in higher volume experiments. The protocol was used in a cell experiment, to research the cell morphological changes of endothelial cells under high physiologically relevant shear stresses. Here, cells tended to orient themselves in the direction of the applied WSS. In higher volume experiments, such as the performed cell experiment, a recirculation pump would be more practical. This, to minimize the volume of used fluid, such as medium, or the needed labour to reuse the fluid.

7 Acknowledgements

Laura de Heus for being daily supervisor in the last six weeks of the bachelor assignment, providing feedback and providing required materials for the experiments.
Jim Koldenhof for being daily supervisor in the first four weeks of the bachelor assignment, introducing me on the AST labspaces and providing his immunohistochemistery data.
dr. Andries van der Meer for being committee chair and providing feedback.
dr.ir. Jeroen Rouwkema for being external committee member.

References

1. Cochrane A, Albers HJ, Passier R, Mummery CL, Berg A van den, Orlova VV, and Meer AD van der. Advanced in vitro models of vascular biology: Human induced pluripotent stem cells and organ-on-chip technology. 2019 Feb. DOI: 10.1016/j.addr.2018.06.007
2. Jeon JS, Bersini S, Gilardi M, Dubini G, Charest JL, Moretti M, and Kamm RD. Human 3D vascularized organotypic microfluidic assays to study breast cancer cell extravasation. Proceedings of the National Academy of Sciences of the United States of America 2015 Jan; 112:214–9. DOI: 10.1073/pnas.1417115112. Available from: www.pnas.org/cgi/doi/10.1073/pnas.1501426112www.pnas.org
3. De Graaf MN, Cochrane A, Van Den Hil FE, Buijsman W, Van Der Meer AD, Van Den Berg A, Mummery CL, and Orlova VV. Scalable microphysiological system to model three-dimensional blood vessels. APL Bioengineering 2019 Jun; 3:026105. DOI: 10.1063/1.5090986. Available from: http://aip.scitation.org/doi/10.1063/1.5090986
4. Bischel LL, Lee SH, and Beebe DJ. A Practical method for patterning lumens through ECM hydrogels via viscous finger patterning. Journal of Laboratory Automation 2012 Apr; 17:96–103. DOI: 10.1177/2211068211426694. Available from: /pmc/articles/PMC3397721/%20/pmc/articles/PMC3397721/?report=abstract%20https://www.ncbi.nlm.nih.gov/pmc/articles/PMC3397721/
5. Katritsis D, Kaiktsis L, Chaniotis A, Pantos J, Efstathopoulos EP, and Marmarelis V. Wall Shear Stress: Theoretical Considerations and Methods of Measurement. Progress in Cardiovascular Diseases 2007 Mar; 49:307–29. DOI: 10.1016/j.pcad.2006.11.001
6. Blood Vessels. Available from: http://droualb.faculty.mjc.edu/Lecture%20Notes/Unit%204/cardiovascular-blood%20vessels%20with%20figures.htm
7. Herland A, Meer AD van der, FitzGerald EA, Park TE, Sleeboom JJF, and Ingber DE. Distinct Contributions of Astrocytes and Pericytes to Neuroinflammation Identified in a 3D Human Blood-Brain Barrier on a Chip. PLOS ONE 2016 Mar; 11. Ed. by Deli MA:e0150360. DOI: 10.1371/journal.pone.0150360. Available from: https://dx.plos.org/10.1371/journal.pone.0150360
8. Marieb EN and Hoehn K. Tissue: The living fabric. *Human Anatomy and Physiology*. 10th ed. Pearson. Chap. 4:135–69
9. Marieb EN and Hoehn K. The Cardiovascular System: Blood Vessels. *Human Anatomy and Physiology*. 10th ed. Pearson. Chap. 19:719–76
10. Cahill PA and Redmond EM. Vascular endothelium - Gatekeeper of vessel health. 2016 May. DOI: 10.1016/j.atherosclerosis.2016.03.007. Available from: /pmc/articles/PMC6478391/%20/pmc/articles/PMC6478391/?report=abstract%20https://www.ncbi.nlm.nih.gov/pmc/articles/PMC6478391/
11. Nigro P, Abe JI, and Berk BC. Flow shear stress and atherosclerosis: A matter of site specificity. 2011 Sep. DOI: 10.1089/ars.2010.3679. Available from: /pmc/articles/PMC3144425/%20/pmc/articles/PMC3144425/?report=abstract%20https://www.ncbi.nlm.nih.gov/pmc/articles/PMC3144425/
12. Selvaganapathy PR. Polymers. *Comprehensive Microsystems*. Vol. 1. Elsevier, 2007 Jan :75–105. DOI: 10.1016/B978-044452190-3.00004-5
13. Qian Z, Ross D, Jia W, Xing Q, and Zhao F. Bioactive polydimethylsiloxane surface for optimal human mesenchymal stem cell sheet culture. Bioactive Materials 2018 Jun; 3:167–73. DOI: 10.1016/j.bioactmat.2018.01.005

14. Falkovich G. Basic equations and steady flows. *Fluid Mechanics*. Cambridge University Press, 2012 Jun :1–53. DOI: 10.1017/cbo9780511794353.003. Available from: https://www.cambridge.org/core/books/fluid-mechanics/basic-equations-and-steady-flows/22E8D275D2B67490C5E0B540C3CC5694

15. Eynolds OR. XXIX. An experimental investigation of the circumstances which determine whether the motion of water shall be direct or sinuous, and of the law of resistance in parallel channels. Philosophical Transactions of the Royal Society of London 1883 Dec; 174:935–82. DOI: 10.1098/rstl.1883.0029. Available from: https://royalsocietypublishing.org/

16. Riveros A, Cuellar M, Sánchez PF, Muñoz-Camargo C, Cruz JC, Sandoval N, Lopez Mejia OD, and Briceño JC. Design and Characterization of a Fluidic Device for the Evaluation of SIS-Based Vascular Grafts. Processes 2020 Sep; 8:1198. DOI: 10.3390/pr8091198. Available from: https://www.mdpi.com/2227-9717/8/9/1198

17. Moses SR, Adorno JJ, Palmer AF, and Song JW. Vessel-on-a-chip models for studying microvascular physiology, transport, and function in vitro. 2021 Jan. DOI: 10.1152/ajpcell.00355.2020. Available from: https://journals.physiology.org/doi/abs/10.1152/ajpcell.00355.2020

18. Batchelor GK. An Introduction to Fluid Dynamics. Cambridge University Press, 2000 Feb. DOI: 10.1017/cbo9780511800 Available from: https://www.cambridge.org/core/books/an-introduction-to-fluid-dynamics/18AA1576B9C579CE25621E80F9266993

19. Fluid mechanics fundamentals and applications (Boek, 2006) [WorldCat.org]. Available from: https://www.worldcat.org/title/fluid-mechanics-fundamentals-and-applications/oclc/834846067

20. Flow Control in Microfluidics– Darwin Microfluidics. Available from: https://darwin-microfluidics.com/blogs/reviews/flow-control-in-microfluidics

21. Walker GM and Beebe DJ. A passive pumping method for microfluidic devices. Lab on a Chip 2002 Aug; 2:131–4. DOI: 10.1039/b204381e. Available from: https://pubs.rsc.org/en/content/articlehtml/2002/lc/b204381e%20https://pubs.rsc.org/en/content/articlelanding/2002/lc/b204381e

22. Hydrostatics. Available from: http://mysite.du.edu/~jcalvert/tech/fluids/hydstat.htm

23. Flow control in microfluidic devices. Tech. rep. Available from: www.elveflow.com

24. Kim S, Lee H, Chung M, and Jeon NL. Engineering of functional, perfusable 3D microvascular networks on a chip. Lab on a Chip 2013 Mar; 13:1489–500. DOI: 10.1039/c3lc41320a. Available from: www.rsc.org/loc

25. Wang L, Wu S, Cao G, Fan Y, Dunne N, and Li X. Biomechanical studies on biomaterial degradation and co-cultured cells: mechanisms, potential applications, challenges and prospects. Journal of Materials Chemistry B 2019; 7:7439–59. DOI: 10.1039/c9tb01539f

26. Mattsson EJ, Kohler TR, Vergel SM, and Clowes AW. Increased blood flow induces regression of intimal hyperplasia. Arteriosclerosis, Thrombosis, and Vascular Biology 1997; 17:2245–9. DOI: 10.1161/01.ATV.17.10.2245. Available from: http://ahajournals.org

27. Davies PF. Hemodynamic shear stress and the endothelium in cardiovascular pathophysiology. 2009. DOI: 10.1038/ncpcardio1397. Available from: /pmc/articles/PMC2851404/%20/pmc/articles/PMC2851404/?report=abstract%20https://www.ncbi.nlm.nih.gov/pmc/articles/PMC2851404/

28. Girard PR and Nerem RM. Shear stress modulates endothelial cell morphology and F-actin organization through the regulation of focal adhesion-associated proteins. Journal of Cellular Physiology 1995 Apr; 163:179–93. DOI: 10.1002/jcp.1041630121. Available from: https://onlinelibrary-wiley-com.ezproxy2.utwente.nl/doi/full/10.1002/jcp.1041630121%20https://onlinelibrary-wiley-com.ezproxy2.utwente.nl/doi/abs/10.1002/jcp.1041630121%20https://onlinelibrary-wiley-com.ezproxy2.utwente.nl/doi/10.1002/jcp.1041630121

29. Butcher DT, Alliston T, and Weaver VM. A tense situation: Forcing tumour progression. 2009 Feb. DOI: 10.1038/nrc2544. Available from: https://www.nature.com/articles/nrc2544

30. Caolo V, Peacock HM, Kasaai B, Swennen G, Gordon E, Claesson-Welsh L, Post MJ, Verhamme P, and Jones EA. Shear stress and VE-cadherin the molecular mechanism of vascular fusion. Arteriosclerosis, Thrombosis, and Vascular Biology 2018; 38:2174–83. DOI: 10.1161/ATVBAHA.118.310823. Available from: https://www.ahajournals.org/doi/suppl/10.1161/ATVBAHA.118.310823.

31. Optimal Therapeutic Formulation — Intrinsic Viscosity Measurements. Available from: https://www.rheosense.com/application-brief-5-intrinsic-viscosity-therapeutic-formulations

32. Cucina A, Sterpetti AV, Pupelis G, Fragale A, Lepidi S, Cavallaro A, Giustiniani Q, Santoro L, and Angelo D'. Shear Stress Induces Changes in the Morphology and Cytoskeleton Organisation of Arterial Endothelial Cells. Tech. rep. 1995 :86–92

33. Silvani G, Romanov V, Cox CD, and Martinac B. Biomechanical characterization of endothelial cells exposed to shear stress using acoustic force spectroscopy 2. bioRxiv 2020 Sep :2020.09.29.319772. DOI: 10.1101/2020.09.29.319772. Available from: https://doi.org/10.1101/2020.09.29.319772

34. Chuah YJ, Koh YT, Lim K, Menon NV, Wu Y, and Kang Y. Simple surface engineering of polydimethylsiloxane with polydopamine for stabilized mesenchymal stem cell adhesion and multipotency. Scientific Reports 2015 Dec; 5:1–12. DOI: 10.1038/srep18162. Available from: www.nature.com/scientificreports

35. Shayegan M and Forde NR. Microrheological Characterization of Collagen Systems: From Molecular Solutions to Fibrillar Gels. PLoS ONE 2013 Aug; 8:e70590. DOI: 10.1371/journal.pone.0070590. Available from: www.plosone.org

36. Jiménez-Torres JA, Peery SL, Sung KE, and Beebe DJ. LumeNEXT: A Practical Method to Pattern Luminal Structures in ECM Gels. Advanced Healthcare Materials 2016 Jan; 5:198–204. DOI: 10.1002/adhm.201500608. Available from: /pmc/articles/PMC4776323/%20https://www.ncbi.nlm.nih.gov/pmc/articles/PMC4776323/

37. Peristaltic pump compared to pressure driven flow control - Elveflow. Available from: https://www.elveflow.com/microfluidic-applications/setup-microfluidic-flow-control/peristaltic-pump-compared-to-pressure-driven-flow-control/

38. Fundamentals of heat and mass transfer. (Boek, 2011) [WorldCat.org]. Available from: https://www.worldcat.org/title/fundamentals-of-heat-and-mass-transfer/oclc/713621645

39. Miyazaki K, Hashimoto K, Sato M, Watanabe M, Tomikawa N, Kanno S, Kawasaki Y, Momoi N, and Hosoya M. Establishment of a method for evaluating endothelial cell injury by TNF-α in vitro for clarifying the pathophysiology of virus-associated acute encephalopathy. Pediatric Research 2017 Jun; 81:942–7. DOI: 10.1038/pr.2017.28. Available from: https://www.nature.com/articles/pr201728

40. Pacher P, Nivorozhkin A, and Szabó C. Therapeutic effects of xanthine oxidase inhibitors: Renaissance half a century after the discovery of allopurinol. 2006 Mar. DOI: 10.1124/pr.58.1.6. Available from: /pmc/articles/PMC2233605/%20/pmc/articles/PMC2233605/?report=abstract%20https://www.ncbi.nlm.nih.gov/pmc/articles/PMC2233605/

8 Appendix

8.1 Protocol: Applying flow in 3D vessel-on-a-chip systems

8.1.1 Materials

- Syringe 5 mL (BD plastipak)
- Syringe Pump (Harvard Apparatus pHd Ultra)
- Microfluidic tubing ø1 mm
- Blunt needle ø1 mm
- Ethanol 70%
- 1X PBS
- Medium
- Viscous finger patterned microfluidic chips
- Pipette tips 200 μL
- Pipette 200 μL

8.1.2 Procedure

1. Connect the 5mL syringe to the microfluidic tubing by pushing one of the open ends of the tubing over the spout of the syringe in a twisting motion.
2. Insert the blunt needle in the other end of the microfluidic tubing.
3. Disinfect the syringe by filling it with 70% ethanol and pushing it through the system by compressing the plunger. After this, clean the blunt needle with ethanol.
4. Fill the syringe for ¼ with PBS by placing the blunt needle in the PBS container and pulling on the plunger. Avoid getting air in the syringe. This air is compressible and might induce pulsatile flow behaviour.
5. Place the syringe on the syringe pump and attach it tightly according to the manual of the manufacturer.
6. Remove one of the pipette tips that sits in the inlet of the microfluidic channel and insert the blunt needle. Do not cover top of the pipette with a finger to avoid pushing air into the channel.
7. Calculate the needed amount of medium. This is the flow rate times the duration of the experiment. To avoid sucking air into the channel, add 10-20% buffer to this amount. The amount is limited at 200 μL, because this is the maximum volume of the pipette.
8. Pipette the needed amount of medium and remove the pipette at the other side of the channel. Place the pipette with medium in the open inlet. Do not press the button to inject fluid into the channel. Carefully release the pipette tip from the pipette.
9. Set the syringe pump to the desired flow rate and execute the experiment.
10. After the flow experiment, pipette 25μL medium in the pipette that sits in the inlet.
11. Remove the blunt needle from the inlet. Fluid will flow from the pipette to the open inlet, this way no air will enter the channel.
12. Pipette 25μL of medium, insert the pipette in the open channel and, as in step 8, carefully release the pipette.

8.2 MATLAB scripts

8.2.1 Lumen width analysis

```
clc;
close all;  % Close all figures (except those of imtool.)
imtool close all;  % Close all imtool figures if you have the Image Processing Toolbox.
clear;  % Erase all existing variables. Or clearvars if you want.
workspace;  % Make sure the workspace panel is showing.
format long g;
format compact;
% Directory of specific folder with images
% Select folder
selpath = uigetdir();
% List with all .tif files from the selected folder.
fileList = dir(fullfile(selpath, '*.tif')); % Change .jpg to .tiff if needed!!
% define outputmatrix with output results in alphabetic order
outcome=zeros(length(fileList),1);
for k=1:length(fileList)
    grayImage=imread(fullfile(selpath,fileList(k).name));
    %grayImage = imread('pout.tif');
    i=1;
    while i==1
        imshow(grayImage);
        % Enlarge figure to full screen.
        set(gcf, 'units','normalized','outerposition',[0 0 1 1]);
        % Give a name to the title bar.
        set(gcf,'name','Select upper wall and bottom wall lumen','numbertitle','off')
        [rows, columns] = size(grayImage);

        % Select the walls of the lumen
        message = sprintf('Click and drag the endpoints of the line\nand double-click the double arrows to finish.');
        uiwait(helpdlg(message));
        h = imline;
        lineEndPoints = wait(h);
        delete h;
        x1 = lineEndPoints(1,1);
        y1 = lineEndPoints(1,2);
        x2 = lineEndPoints(2,1);
        y2 = lineEndPoints(2,2);
        hold on
        plot([x1,x2],[y1,y2], 'r-', 'LineWidth',1); % Make line.
        plot([x1,x2],[y1,y2], 'yo', 'LineWidth',1,'MarkerSize', 5); % Make circles.
        message = sprintf('Click a third point.');
        uiwait(helpdlg(message));
        [x3, y3] = ginput(1);
        plot(x3, y3,'yo','MarkerSize', 5);
        % Calculate the slope.
        slope = (y2 - y1)/ (x2 - x1);
        % Draw second line.
```

```
        x4=x1;
        x5=x2;
        y4 = slope * (x4 - x3) + y3;
        y5 = slope * (x5 - x3) + y3;
        plot([x4,x5 ],[y4,y5],'r-','LineWidth', 1);
        choice = questdlg('Ben je tevreden?','Klopt dit?','Yes','No','Yes');
        % Handle response
        switch choice
            case 'Yes'
                i=2;
            case 'No'
        end
    end
    % Now, determine minimal distance between 2 line segments using function
    % DistBetween2Segment
    p1 = [x1 y1 0]; %p1-4 are endpoints of both lines; input for function
    p2 = [x2 y2 0];
    p3 = [x4 y4 0];
    p4 = [x5 y5 0];
    pd=1000/300;    %pd=pixel to distance ratio (depends on magnification of
       microscope: 1000 um = 300 pixels at 2x (Nikon-ML1))
    fileList(k).lumenwidth_pixels=DistBetween2Segment(p1, p2, p3, p4);
    fileList(k).lumenwidth_um_2xobjective=fileList(k).lumenwidth_pixels*pd;
end
% header={'FileName','Lumen [Pixel]','Lumen [um]'};
filename = 'Lumenwidth.csv';
Output = struct2table(fileList); % Creates a table from the structure (which is
   data type of fileList)
writetable(Output(:,[1,7,8]),fullfile(selpath,filename));%,'LumenWidth.xlsx']));
```

8.2.2 Flow profile plotting

```
clear all

dbstop if error
Q = [flowrate in mL/min] *1.667*10^(-11); %flowrate in m^3/s
mu=0.89*10^(-3);     %viscosity of the fluid in Pa*s
R= [radius in micron] *10^(-6)/2;  %Radius of the vessel in m
L=1*10^(-3);     % length of the vessel in m
dP= (8*mu*L*Q)/(pi*R^4) ;    %pressure drop over the channel in Pa
if dP==0
    disp(' Warning : No flow because the pressure is the whole same in the pipe');
    exit;
end
N=1000;        %Number of used data points
r=linspace(-R,R,N)*10^6;
S=pi*R^2;
Vmean=Q/S;
V=-(dP*((r./10^6).^2-R^2))/(4*mu*L)*10^(3);

%DATA VELOCITY MEASUREMENTS:
Height1 = [First 15 datapoints(distance from bottom wall in micron)]-R*10^6; %
   Distance from center of vessel

```

```
Height2=[Last 15 datapoints(distance from bottom wall in micron)]-R*10^6; % Distance from center of vessel

Speed1 = [First 15 datapoints(bead velocity in micron/s)]*10^(-3); %Velocity in mm/s

Speed2 =[Last 15 datapoints(bead velocity in micron/s)]*10^(-3); %Velocity in mm/s

% FIGURE(1) :
figure(1),
hold on
plot(r,V,'k','LineWidth',2);
plot(Height1,Speed1,'.','Color','r','MarkerSize',35)
plot(Height2,Speed2,'.','Color','b','MarkerSize',35)
hold off
grid on, xlabel('Distance from vessel center(m)'), ylabel('Velocity (mm/s)'), title('Velocity profile at 5 L/min flowrate');
legend('Calculated velocity profile','Bead velocity (frame 414 and 415)','Bead velocity (frame 1003 and 1004)')
```

8.2.3 Video processing

```
function BeadTracking()
% Create System objects used for reading video, detecting moving objects,
% and displaying the results.
obj = setupSystemObjects();
% Create and open a video writer to obtain a video of the mask for further
% analysis
v = VideoWriter('');
open(v)
% Detect moving objects, and track them across video frames.
while hasFrame(obj.reader)
    frame = readFrame(obj.reader);
    [centroids, bboxes, mask] = detectObjects(frame);

    displayTrackingResults();
% Write the frame of the video to the video writer
    writeVideo(v,mask)
end

function obj = setupSystemObjects()
        % Initialize Video I/O
        % Create objects for reading a video from a file, drawing the tracked
        % objects in each frame, and playing the video.

        % Create a video reader.
        obj.reader = VideoReader('');

        % Create two video players, one to display the video,
        % and one to display the foreground mask.
        obj.maskPlayer = vision.VideoPlayer('Position', [740, 400, 700, 400]);
        obj.videoPlayer = vision.VideoPlayer('Position', [20, 400, 700, 400]);

        % Create System objects for foreground detection and blob analysis
```

```
33
34          obj.detector = vision.ForegroundDetector('NumGaussians', 5, ...
35              'NumTrainingFrames', 100, 'MinimumBackgroundRatio', 0.7);
36
37          obj.blobAnalyser = vision.BlobAnalysis('BoundingBoxOutputPort', true, ...
38              'AreaOutputPort', true, 'CentroidOutputPort', true, ...
39              'MinimumBlobArea', 5);
40  end
41
42  function [centroids, bboxes, mask] = detectObjects(frame)
43
44          % Detect foreground.
45          mask = obj.detector.step(frame);
46
47          % Apply morphological operations to remove noise and fill in holes.
48          mask = imopen(mask, strel('rectangle', [3,3]));
49          mask = imclose(mask, strel('rectangle', [15, 15]));
50          mask = imfill(mask, 'holes');
51
52          % Perform blob analysis to find connected components.
53          [~, centroids, bboxes] = obj.blobAnalyser.step(mask);
54  end
55
56   function displayTrackingResults()
57          % Convert the frame and the mask to uint8 RGB.
58          frame = im2uint8(frame);
59          mask = uint8(repmat(mask, [1, 1, 3])) .* 255;
60
61          % Display the mask and the frame.
62          obj.maskPlayer.step(mask);
63          obj.videoPlayer.step(frame);
64   end
65  close(v) %export video of moving beads for analysis
66  end
```

8.3 Data analysis immunohistochemistery in 3D vessel-on-a-chip systems

Background

After a vessel-on-a-chip is produced and seeded, experiments can be performed on it. To get familiar with the processing of data generated by such experiments, data generated by one of researchers at AST, Jim Koldenhof, has been reviewed.

His research looks into the effect of xanthine oxidase inhibitors in combination with certain concentrations of uric acid on the confluence of the lumen. Xantine oxidase inhibitors reduce the production of uric acid and are used as treatment for hyperucemia. *In vivo* hyperucemia leads to endothelial dysfunction, which progresses to endothelial damage.[40]

Method

Immunohistochemistry including F-actin was used to analyse the lumens on macro level to quantify the damage induced by the administered chemicals.

The F-actin images were loaded into Cellprofiler software to compare lumens. The intensity of the locations with F-actin, thus containing endothelial cells, were determined and locations with a value lower were assumed to be without cells in the monolayer. Outlines of the lumens were traced and the image was compared with the lumen if it were perfectly confluent. This way a value between 0 an 1 was obtained. This value is called the rand overlap index of the lumen, with 1 for a confluent cell layer and 0 when there were no cells detected.

After analysis of the images in Cellprofiler and calculating the rand overlap index by Jim, inconclusive results were obtained. All datasets were used without application of statistics to remove outliers.

Dataset analysis

As part of this bachelor assignment another review on the datasets was performed. Firstly, the negative control group, medium, was checked. It is expected that, when medium is provided to the cells, no degradation of the cell layer will occur. Therefore, all datasets with values for the overlap rand index lower than 0.95 were excluded. This resulted in only two usable datasets on which still no strong conclusions could be based. Secondly, the positive control group, TNF-α, suggests great degradation of the cell layer. However, no such effect was observed. Lastly, to rule out problems in the used Cellprofiler quantification method a few images were manually compared to each other. In figure 12 two compared images are shown. Figure 12a and 12b were by image processing in Cellprofiler given a overlap rand index of 0.60 and 0.68 respectively. However, when looking at these images side by side, the channel in figure 12a shows a higher overall F-actin intensity in respect to the channel in figure 12b. This questions the used quantification method and has to be investigated further.

Recommendations

Due to a shortage in time, no further images were manually analysed to verify the overlap rand index. For further data processing it is recommended to compare images of each condition and the corresponding overlap rand index side by side to check for further remarkable value-image combinations. This way specific outliers can be excluded from the data.

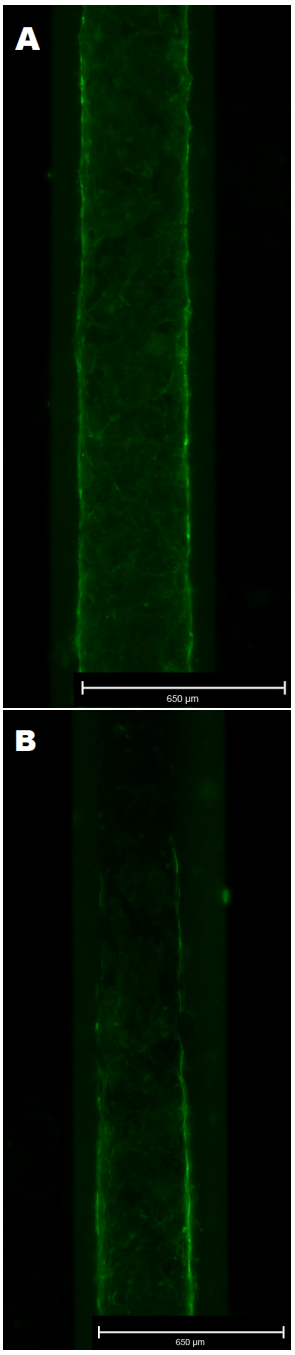

Figure 12: Two immunohistochemistry images showing F-actin staining. (A) overlap rand index of 0.60 and (B) overlap rand index of 0.68.